

Synchrotron Techniques for In Situ Catalytic Studies: Capabilities, Challenges, and Opportunities

Anatoly I. Frenkel,^{*,†} Jose A. Rodriguez,^{*,‡} and Jingguang G. Chen^{*,§,||}

[†]Department of Physics, Yeshiva University, New York, New York 10016, United States

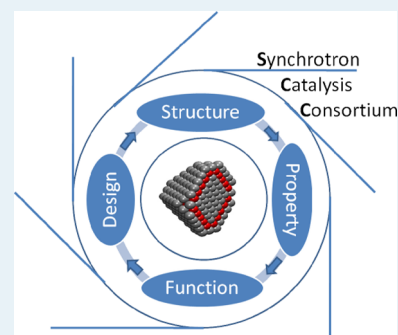
[‡]Department of Chemistry, Brookhaven National Laboratory, Upton, New York 11973, United States

[§]Department of Chemical Engineering, University of Delaware, Newark, Delaware 19716, United States

^{||}Department of Chemical Engineering, Columbia University, New York, New York 10027, United States

ABSTRACT: Most industrial catalysts are complex materials that usually operate at elevated pressures and temperatures. Pressure, materials, instrument, and complexity gaps are obstacles toward understanding how catalysts work and how to rationally design new catalysts. In this article, we examine existing and emerging approaches to bridge some of these gaps and gain new insights into the catalyst active phase and catalytic mechanism using synchrotron-based spectroscopy, scattering, and imaging methods. The utilization of in situ, time-resolved synchrotron techniques offers unique opportunities to study working (operando) catalysts. Using several representative examples from recent literature we illustrate the synergy from using combinations of techniques to identify new details about catalytic properties that are unavailable when these methods are used separately. Following this approach it is possible to identify new catalyst phases and reaction intermediates.

KEYWORDS: synchrotron, in situ, operando, catalysis, EXAFS, XRD



1. INTRODUCTION

Since their inception, synchrotron radiation sources have been attracting an ever growing number of catalysis scientists. Almost every major synchrotron facility has an active catalysis research community among its users. Recent reviews describe the broad range of tools, from spectroscopy^{1,2} to scattering^{3,4} to imaging,^{5,6} available for catalysis investigations using synchrotron radiation. In principle, one must be able to characterize complex materials that operate in a wide range of temperature and pressure conditions.^{1–6} Because of the complexity of interactions occurring simultaneously in broad spatial and temporal ranges, this field relies not on a single instrument or single experiment, but on a combination of information gained from different sources. Significant progress has been made in the past two decades in transforming a typical synchrotron hutch into a modern day chemistry laboratory with a hub of integrated instruments, as illustrated in the following examples. Clausen et al.⁷ reported the first combination of synchrotron X-ray absorption spectroscopy (XAS) and X-ray diffraction (XRD) for in situ studies of catalysts almost 20 years ago in HASYLAB at DESY (Hamburg, Germany). The field has been continuously advanced ever since, to its present state where the XAS, in particular extended X-ray absorption fine structure (EXAFS), and XRD measurements are applied for investigations of working catalytic processes, that is, in operando.^{8–11} Several authors have further enhanced the combined measurements by adding complementary electronic and vibrational spectroscopy techniques, including ultraviolet-visible (UV–vis.), infrared (IR), and Raman, to the well established

XAS-XRD combination.^{12–16} Weckhuysen and others have combined the small and wide angle scattering (SAXS and WAXS) techniques with quick-scanning EXAFS (QEXAFS) to study in situ processes.^{14,17} Newton et al. began to explore the analytical power of the combinations of Diffuse Reflectance Infrared Fourier Transform Spectroscopy (DRIFTS) with time-resolved XAS,^{18–20} and time-resolved XRD.²¹ Newton and Chupas have advanced the XRD-pair distribution function (PDF) methods for in situ and operando catalysis studies.^{22,23} More details about some of these advances can be found in a recent review by Bentrup.²⁴

The progress in synchrotron catalysis methods would not be possible without the development of in situ and operando reactors for homogeneous and heterogeneous catalysis that couple synchrotron techniques (XAS and XRD) with vibrational spectroscopies.^{13,16,25–29} The opposite can be also true: invention of the quick scanning (QEXAFS) monochromator was motivated by specific needs of catalysis science, namely, to study reaction kinetics with subsecond time resolution. QEXAFS applications extend now to problems in environmental and materials sciences, that is, far beyond the realm of catalysis.^{30,31} The millisecond time barrier will be inevitably broken by using microfluidic reactors for XAS.³² Nanometer-resolution imaging and tomography studies of catalytic

Special Issue: Operando and In Situ Studies of Catalysis

Received: June 20, 2012

Revised: August 26, 2012

Published: September 17, 2012

processes in real time are now possible because of the better focusing optics, nanometer-precision positioning stages, and nanoreactor technologies.³³

Continuing improvement in spatiotemporal resolution imposes constraints on the experimental geometry (e.g., small working distance between the sample and the detector, or the micrometer size reactors), thus complicating the integration of the new generation of in situ instruments in the same experiment. It is, therefore, timely to revisit the main rationale for this approach that was successfully used for two decades. In this Perspective we will critically review the new type of information that emerges from combining different methods to study catalytic processes at synchrotrons in operando. We will begin with several examples showing how the nature of active site in the water-gas shift (WGS) reaction can be refined by combining XAS data with simultaneous product analysis. In the subsequent sections, we will focus on the combination of the XAS and X-ray scattering-based methods and their coupling with other operando studies. Many examples are taken from the authors' own experience at the Synchrotron Catalysis Consortium (SCC) at the National Synchrotron Light Source (NSLS) of Brookhaven National Laboratory. When describing X-ray spectroscopy we limit the discussion to the "tender"-to-hard X-ray energy range, typically from 2 KeV and above. Readers interested in learning more about the methods available for catalytic studies utilizing ultraviolet and soft X-ray ranges of synchrotron radiation are referred to excellent reviews on these subjects.^{5,34–36}

2. USING XAS TO DETERMINE ACTIVE SITES

2.1. Catalysis. One example of the application of XAS to heterogeneous catalysis comes from studies of the active phase for metal/oxide catalysts used for the WGS reaction. The nature of the active phase(s) in metal/oxide WGS catalysts and the WGS reaction mechanism is a matter of ongoing debates.³⁷ Thus, XAS was used to obtain a systematic understanding of the structural, electronic, and chemical properties of CuO/CeO₂, Ce_{1-x}Cu_xO₂, CeO_{2-x}/CuO, and AuO_x/CeO₂ WGS catalysts.^{38–43} For example, the as-prepared AuO_x-CeO₂ catalysts contain nanoparticles of pure gold and gold oxides dispersed on a nanoceria support.⁴⁴ Each of these gold species could be in the active phase, and the ceria support may not be a simple spectator in these systems.^{37,44} The top panel in Figure 1 shows data for the production of H₂ and CO₂ during the WGS over a powder gold-ceria catalyst,³⁹ with the catalyst being held at reaction temperatures of 300, 400, and 500 °C. The experimental setup did not detect significant catalytic activity at temperatures below 250 °C.³⁹ The chemical state of gold during the WGS was determined by means of in situ, time-resolved X-ray absorption near-edge structure (XANES). The bottom panel in Figure 1 displays Au L₃-edge XANES spectra collected at room temperature for fresh catalysts with a Au content of 0.5 wt % (dashed trace) or 2.4 wt % (solid traces). The line shape of these two spectra is very similar and shows a clear feature at ~2.5 eV above the edge that is not seen for metallic gold and is characteristic of gold oxides.^{39,45} A quantitative analysis indicated that the intensity of this peak is higher than that observed for Au₂O and closer to that seen in Au₂O₃.⁴⁵ The intensity of the peak is proportional to the number of electron holes in the valence d band of Au.⁴⁵ Once the 2.4 wt % Au-CeO₂ catalyst was exposed to a mixture of CO/H₂O at elevated temperatures, the XANES features for gold oxide disappeared at temperatures well below 200 °C.³⁹

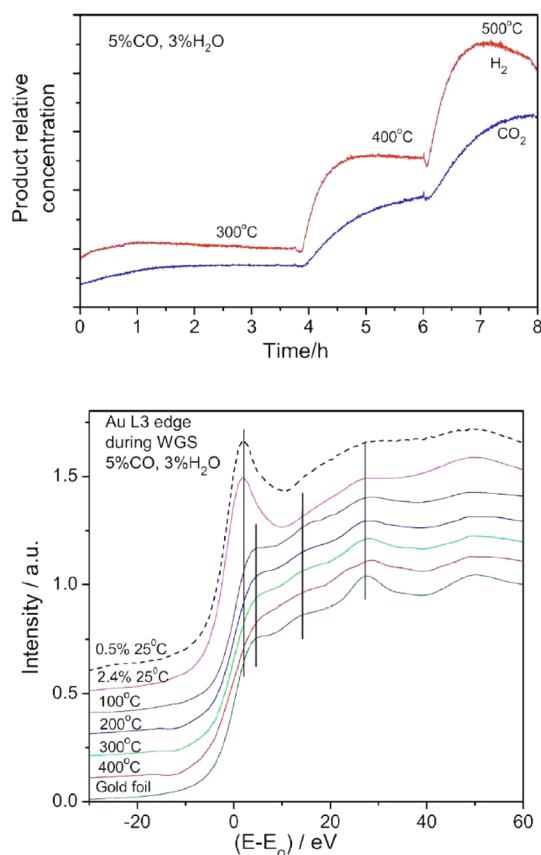


Figure 1. Top panel: Relative amounts of H₂ and CO₂ formed during WGS over a 2.4% weight Au-CeO₂ catalysts. A mixture of 5% CO and 3% H₂O in He (total flow ~10 mL/min) was passed over the catalyst at 300, 400, or 500 °C.³⁹ Bottom panel: Au L₃-edge XANES spectra collected in situ during the WGS reaction over the same catalyst. For comparison, Figure 1 also includes the spectra for a fresh 0.5 wt % Au-CeO₂ catalyst, dashed trace, and a gold foil. The vertical line indicates the main features for AuO_x versus metallic Au. Spectra reprinted with permission from ref 39. Copyright 2005 American Institute of Physics.

Around 150 °C, the Au L₃-edge XANES spectrum of the 2.4 wt % Au-CeO₂ catalyst closely matched the corresponding spectrum for metallic Au. EXAFS data showed the disappearance of the *r* peak for Au-O in AuO_x with the simultaneous appearance of the *r* peak for Au-Au in metallic Au. Thus, at temperatures above 200 °C, when significant WGS activity was detected, the line-shape of the Au L₃-edge indicated the existence of pure gold.³⁹ In situ measurements of the Ce L₃-edge showed that ceria was partially reduced under WGS conditions becoming CeO_{1.95}. The XANES spectra in Figure 1 were obtained under a reaction mixture of 5% CO and 3% H₂O in He (total flow ~10 mL/min).³⁹ Thus, the in situ time-resolved XAS data indicate that cationic Au^{δ+} species *cannot* be the key sites responsible for the WGS activity in Figure 1, because they do not exist under reaction conditions.³⁹ An identical finding has been found in XANES experiments for AuO_x/Ce_{1-x}Zr_xO_{2-y} powder catalysts.³⁷ In these catalysts, the results of XANES measurements at the Au and Ce L₃-edges indicate that the active phase consists of small Au aggregates (<2 nm in size) dispersed on partially reduced ceria (CeO_{1.94}-CeO_{1.98}).^{39,37} The behavior observed for AuO_x/CeO₂ under WGS reaction conditions is not unique. Similar in situ XANES studies for the WGS reaction on CuO/CeO₂, Ce_{1-x}Cu_xO₂ and

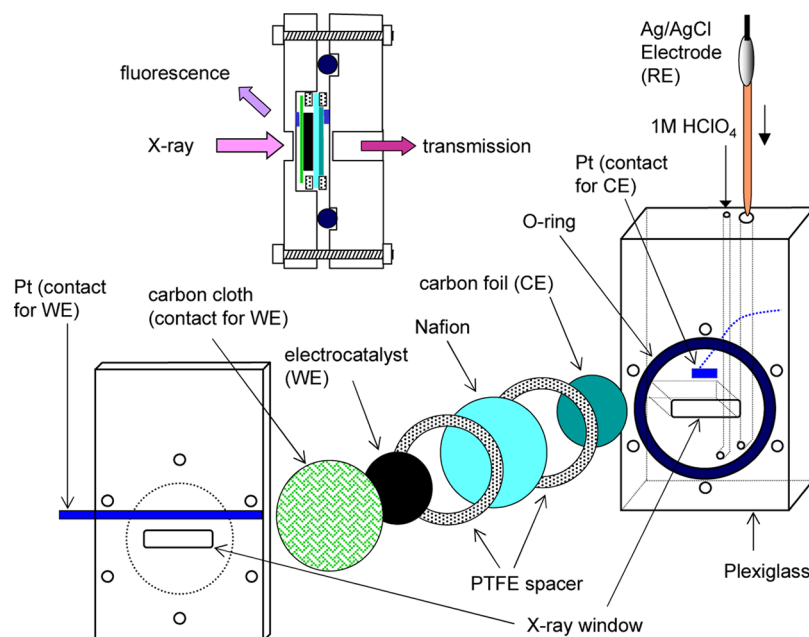


Figure 2. Electrochemical cell for in situ XAS studies designed by the Adzic group.

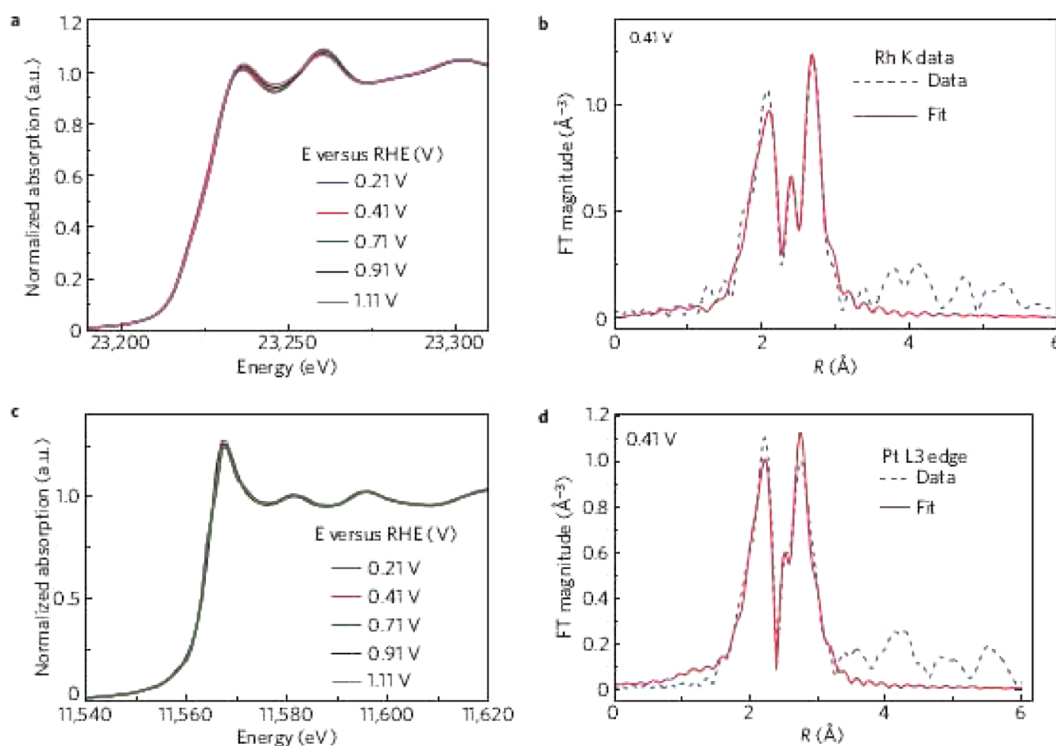


Figure 3. In situ XANES and EXAFS spectra for determining the electronic and structural properties of PtRhSnO₂. XANES spectra (a,c) and Fourier-transform magnitudes (b,d) of the Rh K-edge (a,b) and Pt L_{III}-edge (c,d) for the PtRhSnO₂/C electrocatalyst in 1M HClO₄ solution as a function of half-cell potential. Modified with author permission based on figure in ref 51. Copyright 2009 Nature Publishing Group).

CeO_{2-x}/CuO point to a full reduction of CuO by CO, and metallic Cu appears to be the active phase of these catalysts.^{38,40,46,42} These and similar studies with in situ XANES and XRD^{7–21} indicate that a heterogeneous catalyst is a dynamic entity with properties that change as a function of the reaction conditions.

2.2. Electrocatalysis. Fuel cells, in particular polymer electrode membrane (PEM) fuel cells, are expected to become one of the major alternative sources of energy for stationary and

transportation applications. Despite definitive advances in recent years, one of the major hurdles is the high Pt content in electrocatalysts. The extensive use of XAS under in situ electrochemical conditions has played an important role in developing electrocatalysts with enhanced activity and reduced Pt content. In situ XAS measurements offer the opportunity to study electrocatalysts under operating conditions in electrochemical cells, and to determine the origin of their catalytic activity. The structural and electronic properties determined

using in situ XAS can facilitate reliable structure–activity correlations that potentially offer guidelines for designing new electrocatalysts. The possibility of reproducing the fuel cell conditions is also very useful in identifying the transient phenomena causing degradation of the catalysts.

Figure 2 shows a typical design of a half-cell from the Adzic group,⁴⁷ for in situ studies of electrocatalysts with H₂ and O₂ flows. Such studies are particularly attractive when different electrocatalysts are used at anode and cathode. Such reaction cell allows for the in situ studies at the fuel cell operating temperatures of 60–80 °C. The in situ studies are uniquely suited for correlating XAS spectral information unambiguously with the catalytic activity since all atoms sampled by the X-ray beam are involved in the reaction.⁴⁸ This version has been chosen as the starting point for modified designs by other groups.^{49,50}

For example, the utilization of in situ XAS played a critical role in the explanation of the activity of a ternary PtRhSnO₂/C electrocatalyst that is capable of oxidizing ethanol with high efficiency and showing great promise for breaking the C–C bond in ethanol at room temperature in acid solutions.⁵¹ As shown in Figure 3, the electronic and structural properties of the PtRhSnO₂ electrocatalyst and their potential dependence were determined using in situ XANES and EXAFS. Figures 3a and 3c show the Rh K-edge and Pt L_{III}-edge XANES spectra for PtRhSnO₂/C, respectively, obtained in the potential region from 0.21 to 1.11 V in 1 M HClO₄ solution. The main absorption peaks at the Rh and Pt edges showed very small potential dependence, suggesting that the electrocatalytic surfaces were only slightly oxidized during electrochemical measurements. Furthermore, the metal–metal coordination numbers from the EXAFS analysis (Figures 3b and 3d) were consistent with a homogeneous distribution of Pt and Rh throughout the electrocatalyst particles. The electronic and structural properties derived in Figure 3 provided important insight into the active site for the electrooxidation of ethanol under fuel cell operating conditions.⁵¹

Specifically, as mentioned above, the in situ studies of XANES at different potentials demonstrated that Pt and Rh species are only weakly oxidized at all potentials studied. That was an important observation that helped reveal the role of SnO₂ sites that are saturated by H₂O/OH and weaken the interaction of water with Pt and Rh, thus making them available for ethanol oxidation. The conclusion that both Pt and Rh participate in the reaction, supported also by density functional theory (DFT) calculations, stems in part from EXAFS analysis indicating that both types of atoms are present at the catalyst surface.

In addition to the example of anode electrooxidation catalysts shown in Figure 3, in situ XAS studies have provided important information regarding the active sites and stability of cathode electrocatalysts for the oxygen reduction reaction (ORR),⁵² as well as the structure–property relationship in low-dimensional electrocatalysts, such as monolayers Pt supported on Au and TiO₂.^{53,54} Similar XAS studies should provide insight into the activity and stability of monolayers Pt electrocatalysts for hydrogen evolution reaction (HER) for water electrolysis.⁵⁵ Another opportunity of future XFS research is the investigation of active sites of electrocatalysts in in situ photoelectrochemical cells.⁵⁶

3. COMBINING XAS WITH OTHER TECHNIQUES

3.1. Combining XRD with XAS. The actual structure of the active phase of a catalyst can range from crystalline to amorphous, or mixture of the two.^{57–59} This is a relatively common situation seen in metal/oxide catalysts where the oxide support is mainly crystalline and small metal particles are amorphous. Another example is a reactor compartment that contains a mixture of reduced and unreduced state of the same catalyst. In a common terminology used in crystallography,⁶⁰ the structure of a catalyst can have local, medium, or long-range order. While all solids from crystalline to amorphous have local order, the long-range order exists only in the crystals. Yet, all types of systems may be present in a catalytic system: an ordered structure in an oxide support, a mixture of large crystalline metal clusters, and small, disordered, and/or amorphous ones. To understand the nature of catalytically active phase one should have techniques available to characterize these different degrees of structural order in the working catalyst.

XAS is sensitive to the local structure only, within a few coordination shells around the absorbing atom. For systems with small to moderate disorder, XAS can characterize local structure accurately even if the long-range order is absent. On the other hand, Bragg diffraction originates from coherent scattering and thus requires long-range periodicity within a region at least a few unit cells in size. The formation of strongly disordered and low dimensional phases, as well as metastable reaction intermediates, is a very common phenomenon in catalytic processes.^{57–60}

For samples possessing long-range order, XRD has been one of the most frequently applied techniques in catalyst characterization.⁶¹ Over the past decade researchers have been conducting subminute, time-resolved in situ XRD experiments under a wide variety of temperature and pressure conditions (–190 °C < *T* < 930 °C; *P* < 50 atm).⁶² These advances result from combining the high intensity of synchrotron radiation with new parallel data-collection devices.

The concept of combining synchrotron techniques dates back to the pioneering work of Thomas⁶³ and Clausen.⁷ They combined XRD and XAFS in one single experiment with enough time resolution to follow the kinetics of structural changes of solids under in situ conditions and opened the door to the employment of a powerful characterization tool for unraveling complex structural transformations and its application to mixed oxides systems. Further developments in the technique increased the resolution of both the XRD and XAS measurements. An experimental setup for XAS/XRD has been built at beamline X18A of the NSLS and used to explore the advantages and limitations of the simultaneous utilization of these techniques in measuring structure and kinetics in the same catalytic system.¹¹ Nearly simultaneous XRD and XAFS measurements of the behavior of several catalysts under reducing or oxidizing conditions have been performed.¹¹

The structure and chemical state of an inverse CeO₂/CuO catalyst was investigated under reduction with CO and oxidation with O₂.¹¹ The sample powder was loaded in a 1/8" Kapton tube in a flow cell. XRD patterns (measured with 30 s exposure time) were collected at 20 KeV during reduction by flowing 5% CO/He mixture while increasing the temperature from room temperature (RT) to 200 °C. The XRD was also measured during oxidation experiments, where the 20% O₂/He mixture was introduced at 200 °C, and the temperature was

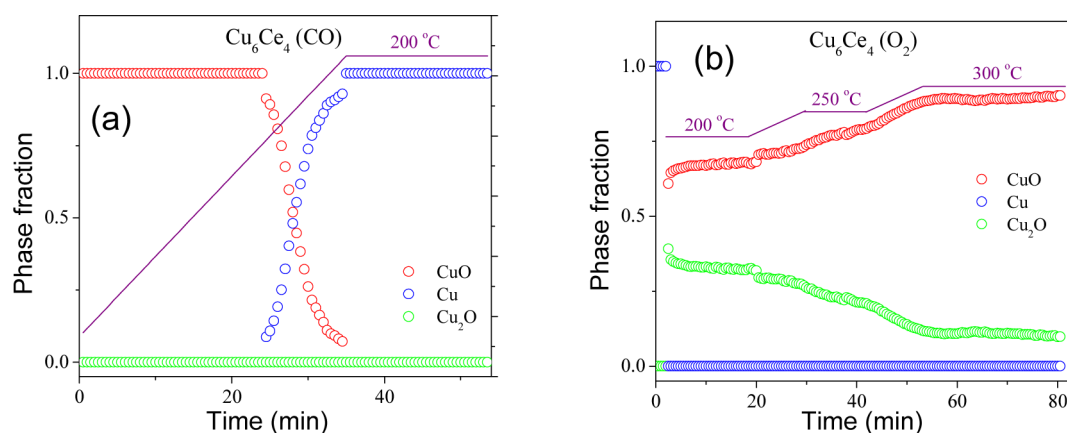


Figure 4. Molar phase fraction of copper species during reduction (a) and reoxidation (b), as measured by the XRD. Reprinted with permission from ref 11. Copyright 2011 American Chemical Society.

Table 1. Mixing Fractions of Cu⁰, Cu⁺, and Cu²⁺ in the Inverse CuO/CeO₂ Catalysts Obtained during CO Reduction and O₂ Oxidation by XAS and XRD Techniques in a Single Experiment¹¹

sample	Cu ⁰		Cu ⁺		Cu ²⁺ in CuO		Cu ²⁺ in CeO ₂	
	XAFS	XRD	XAFS	XRD	XAFS	XRD	XAFS	XRD
fresh	0	0	0	0	73%	90%	27%	10%
reduced at 200 °C	70%	96%	17%	0	13%	0	0	4%
reoxidized at 200 °C	23%	0	30%	31%	47%	67%	0	2%
reoxidized at 300 °C	0	0	0	0	70%	95%	30%	5%

held at 200 °C then increased and held at 250 and 300 °C. EXAFS scans were collected before and after the CO reduction at 25 and 200 °C, as well as during the reoxidation experiment (at the end of the 30 min exposure to O₂) and at 300 °C (after the extended exposure to O₂). Gases leaving the reaction chamber were analyzed with a quadrupole mass spectrometer (QMS).

The Rietveld refinement analysis results of the time-resolved XRD measurements are shown in Figure 4 and Table 1. From Figure 4a it can be seen that no intermediate phase (Cu₂O) was observed in the process of reduction. In Figure 4b, the reoxidation resulted in the mixture of CuO and Cu₂O at 200 °C in 20%O₂/He, and Cu₂O was found to be fully oxidized at 300 °C. The above results demonstrate that, according to XRD, the Cu₂O intermediate structure is only stable in the reoxidation step.

The corresponding Cu K-edge XANES data in Figure 5 (inset) show the transformation of the fresh sample upon CO reduction and subsequent reoxidation. The fresh sample was found to be dominated by Cu²⁺, in agreement with XRD, and the reoxidized sample at 300 °C was found to be identical with the fresh sample in the XANES region (Figure 5). Linear combination fits of XANES data provided the fractions of Cu⁰, Cu⁺, and Cu²⁺ in the reduced and reoxidized samples. For the linear combination analysis the XANES data measured in Cu metal foil, CuO and Cu₂O powder data were used as standards for the Cu⁰, Cu⁺ and Cu²⁺ oxidation states, respectively. In addition, an experimental standard for the substitutional phase Cu:CeO₂ was also used.

Numerical results for the XANES and XRD data analyses are summarized in Table 1. Interestingly, the two techniques reported different amounts of Cu⁰, Cu⁺, and Cu²⁺ in the samples during the reduction and reoxidation processes. In the both cases, XRD underestimated the amounts of *minority* phases in the sample (Cu⁺ and Cu²⁺ in the reduced sample and

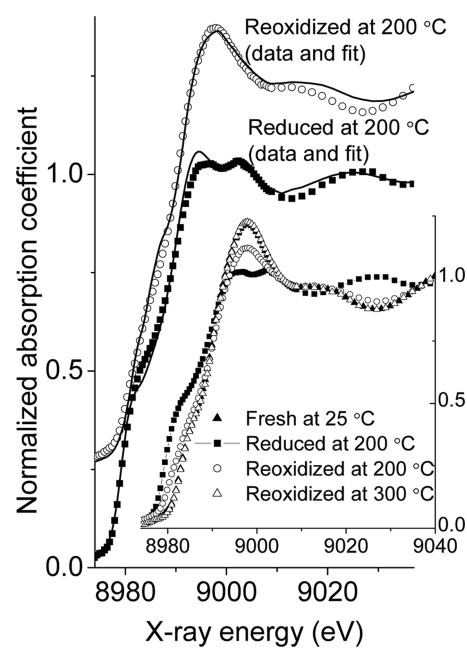


Figure 5. Cu K-edge XANES data and linear combination fits for the Cu/ceria inverse catalyst, reduced (with CO) and reoxidized (with O₂) at 200 °C. Inset shows the raw data obtained at different states of the reaction. Reprinted with permission from ref 11. Copyright 2011 American Chemical Society.

Cu⁰ and Cu⁺ in the oxidized sample). One can conclude that the reduced sensitivity of XRD to these contributions was likely to be caused by the enhanced disorder and/or low dimensionality of these undetected phases. XAS, being a local structural method, is thus more likely to detect such phases. However, without the simultaneous XRD measurement, XAS results would not indicate their disordered nature, that is, the

XAS analysis results would have been incomplete or, worse, even misleading. Only when combining the two measurements together in one self-consistent analysis methodology can the new information about the disordered nature of the transient species be obtained.

A similar conclusion (about the presence of low dimensional phase, invisible to XRD) was obtained in a study of the reduction of a WGS CuFe_2O_4 catalyst in CO.¹¹ For CuFe_2O_4 under reducing conditions, the combined use of XAS and XRD allowed the acquisition of accurate data for the kinetics of nucleation and growth of metallic Cu (Figure 6), the active catalytic phase in the WGS process.

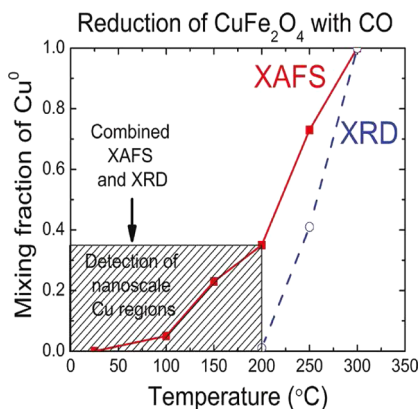


Figure 6. Comparison of the Cu^0 fractions determined by XRD and XAS for the reduction of a WGS CuFe_2O_4 catalysts in CO. Reprinted with permission from ref 11. Copyright 2011 American Chemical Society.

The combination of XAS and XRD measurements in the same experiment puts limitations in the precision of the data that can be obtained with each technique, but this combination is necessary if one wants to explore correlations between the structural and the electronic properties of a catalyst. We will now discuss whether the accuracy of XAS and XRD measurements done in combined mode is adequate for operando investigations. In time-resolved operando experiments the central question in most catalysis studies is: how to extract the information on the reaction kinetics from the available experimental data. The kinetic information most often sought is the studies of reaction intermediates, although the investigation of reaction rates and kinetic barriers is also commonly pursued. To find out the number and the identity of the reaction intermediates, the excellent accuracy of standalone EXAFS and XRD refinements (that can be done by multiple-scattering fit and Rietveld analyses, respectively) is not required. For example, EXAFS fitting analysis would not be conclusive when multiple phases are present because of the large number of structural parameters to refine. Instead, a common alternative is the use of simplified, linear algebra methods: linear combination analysis or principal component analysis, where the phase speciation is done model-independently and reliably, using either XANES or EXAFS spectra or both. Only after the phase speciation is achieved should a refinement of the structure be planned, which is a separate step that does not require a combined investigation; and such structures can be obtained separately by EXAFS and XRD measurements and later accurately refined, which is an established approach.⁴¹

The experimental setup for nearly simultaneous XAS/XRD offers an exciting new possibility to study heterogeneous catalysis by in situ Diffraction Anomalous Fine Structure (DAFS).⁶⁴ This method, combining the long-range order sensitivity of XRD and short-range order specificity of XAS within the same in situ reaction cell, has been used in the past for discriminating between the nanocrystalline and the bulk amorphous phases of the same atomic species.⁶⁵ The XAS/XRD setup allows one to extend these ideas to perform in situ, real time chemical speciation and kinetics studies in the system containing reduced and oxidized states of the same catalyst.¹¹

3.2. Combining Imaging Techniques with XAS: Bridging the Length Scales by Combining Spatially Averaged and Local Studies. Because of the concentration and temperature gradients that can occur during chemical reactions, it is important not only to measure the average information over the large area illuminated by X-ray beam in real time but also to complement it with the local information about the state of the catalyst in each section of the reactor. This can be accomplished by spatially resolved spectroscopy that uses either scanning X-ray microscopy with microfocused X-ray beams or full field X-ray microscopy with X-ray camera.⁶⁶ The second method is often employed in combination with tomographic imaging techniques^{66,67} that allows to reconstruct a three-dimensional structure of the sample. This technique has been recently combined with fluorescence mapping,^{68,69} with⁷⁰ and without⁷¹ energy scanning.

An excellent example of the new information that micro-tomography and micro-X-ray fluorescence imaging provides is the work by Jones et al.⁶⁹ performed at beamlines X26A and X27A of the NSLS. They demonstrated their potentials for monitoring changes in the catalyst composition during Fischer–Tropsch synthesis. Fluorescence microtomography images are shown in Figure 7, top, which demonstrate the nonhomogeneous distribution of Fe atoms within a portion of the sample and the change in Fe distribution during the reaction. Fluorescence maps (Figure 7, bottom) demonstrate relative concentration of each promoter (Fe, Ni, Cu, Zn, and Pb) in one of the analyzed samples. Combined, these data may help understand the mechanisms of catalyst activity, its enhancement due to the presence of additional components, and the catalyst deactivation.

Grunwaldt et al.⁷⁰ demonstrated that new information about catalytic mechanisms can be gained if energy is scanned during the full field microscopy measurements. The new type of data was the spatially resolved valence state of Rh catalyst supported on Al_2O_3 . These data (Figure 8) were measured in operando, during the partial methane oxidation reaction catalyzed by this system. There is a clear advantage of doing such experiments in energy scanning mode vs staying at a single energy corresponding to, for example, white line maximum. When energy is scanned, the spectra can be analyzed either by XANES or EXAFS analysis methods and an important question can be answered about the transformation pathway between different oxidation states of the catalyst: does it go through an intermediate state or states or is it a one-step process between the initial and the final states. Clearly, such question cannot be answered by a single energy measurement, but linear combination of principal component analysis techniques can provide detailed answer when the collection of spectra is measured at different positions in the reactor and/or reaction times.^{72,41,73–75}

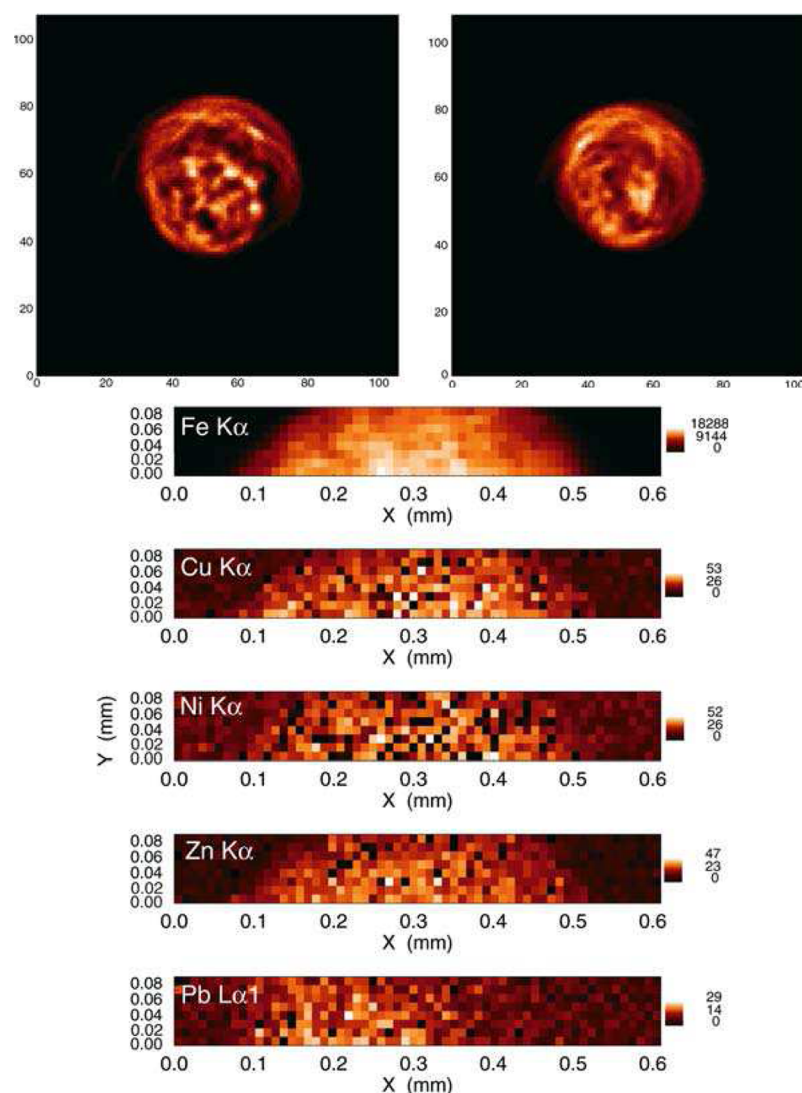


Figure 7. Top: Fe distributions in two fluorescence tomographic sections through the Fischer–Tropsch sample show variability of the catalyst concentrations within the same waxy sample. The pixel size for the images is 0.010 mm \times 0.010 mm (ref 69) Bottom: Maps of Fe, Ni, Cu, Zn, and Pb metals detected in the Fischer–Tropsch waxy sample taken during the reaction. The maps show variability of concentrations on a pixel-to-pixel scale. Reprinted with permission from ref 69. Copyright 2005 Springer Science and Business Media.

3.3. Coupling Spectroscopy and Diffraction to Surface Reactivity Studies. The determination of the active phase of a catalyst is usually followed by experimental and/or theoretical studies on the surface chemistry and reaction mechanism associated with the catalytic process.⁷⁶ The importance of knowing a reaction mechanism is that it often provides a rational way to improve catalytic activity and selectivity.⁷⁷ Ideally, one should be able to monitor simultaneously the changes that occur in the structure of the catalyst particle and the chemical species that are being transformed on the catalyst surface. Understanding of the mechanism for a catalyzed reaction requires direct observation of the chemical species involved in the elementary steps and the kinetics for their transformations.⁷⁷ In recent years, there has been a strong drive toward the integration of techniques that provide information on the structural properties of the catalysts by coupling XRD, XAS with techniques that allow the study of surface reactions, infrared and Raman spectroscopy.

Infrared spectroscopy is perhaps the most commonly used technique in heterogeneous catalysis to identify adsorbed

species and to study the way in which these species are chemisorbed in the surface of the catalyst.⁷⁸ It is a frequently used technique in mechanistic studies,^{6,79–81} having one of the longest histories among the methods for in situ characterization.⁷⁸ When combined with probe molecules (CO, NO, etc), infrared spectroscopy can yield valuable information about the adsorption sites in the catalyst.^{78,80,82–84} Raman spectroscopy has also become popular for in situ studies because it also provides information about the active sites and adsorbed species.^{6,85} Since the selection rules for vibrational transitions are different in infrared and Raman spectroscopies,⁸⁶ the information obtained from the two techniques often complements each other and thus provides valuable structural information.

In recent years different experimental setups have been developed to combine XAS/IR,^{6,87,88} XAS/Raman,^{6,29,87,89} XRD/IR,^{21,87} and XRD/Raman^{6,87,90} opening the door to operando studies of the links between the structural and the chemical properties of heterogeneous catalysts. At beamline X18A of the NSLS a new instrument for synchronous in situ

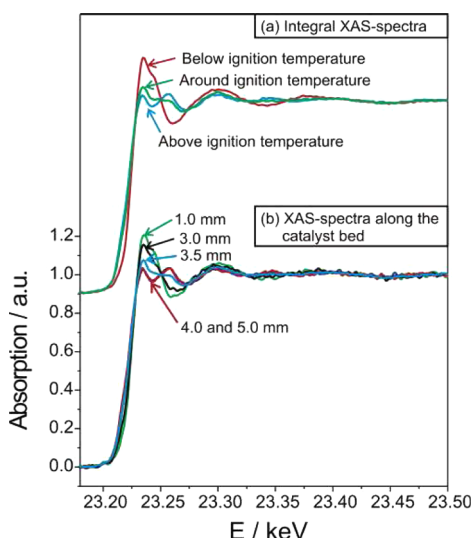


Figure 8. X-ray absorption spectra at the Rh K-edge of the 2.5 wt % Rh/Al₂O₃ catalyst (a) in an integral manner (averaged over the whole sample by wide beams) below, around and above the ignition temperature; (b) in a “local” manner probing at different positions of the catalyst bed with a 1 mm × 0.6 mm X-ray beam at 283 °C. Reprinted from ref 70. Copyright 2006 American Chemical Society.

investigation of catalytic materials by infrared and XAS was designed and built.⁸⁸ Among the features attractive for catalysis research are the broad range of catalytically active elements that can be investigated (all metals), the wide range of reaction conditions (temperatures up to 600 °C, various reactive gases) and time resolution (starting from tens of seconds).⁸⁸

The XAS/IR setup at beamline X18A of the NSLS have been used to study CO oxidation, the synthesis and reforming of alcohols, olefin hydrogenation, and the WGS reaction.⁸⁰ EXAFS and XANES are not particularly efficient techniques for studies of the surface structure of nanoparticle catalysts during their interactions with reactants, for example, adsorbates and ligands attached to the catalyst surface, because their signal is dominated by the absorber atoms inside the nanoparticles. DRIFTS is a useful alternative for such analysis because of the sensitivity on the functional groups adsorbed on the surface of the catalyst.⁸⁸ For example, Figure 9 shows data acquired using

this facility. In situ XANES and DRIFT spectra were collected during the reduction of a Pt/γ-Al₂O₃ catalyst in a 5% H₂/He atmosphere while ramping the temperature from room temperature to 400 °C at a rate of 5 °C min⁻¹.⁸⁸ The reduction of Pt particles is clearly evident in the XANES spectra (Figure 9b) by the decrease in the white line intensity.⁸⁸ DRIFT spectra, recorded simultaneously with XAS, are shown in Figure 9a. Two bands are visible at lower temperatures at 2120 and 2050 cm⁻¹. As the temperature increases, the former band weakens in intensity and eventually disappears from the spectrum around 150 °C, whereas the lower frequency band increases in height and shifts in frequency from 2050 to 2060 cm⁻¹. The highest intensity and the frequency of the latter band are found at 350 °C. A further temperature increase causes the band to decrease in intensity and to shift toward lower wavenumbers. The origin of the higher frequency peak is usually associated with the weak Pt–H vibration, whereas that at 2060 cm⁻¹ is believed to be caused by CO impurities.⁸⁸

X-ray photoelectron spectroscopy (XPS) is another technique that is commonly used in studies of surface reactivity. XPS is a well established technique for the characterization of catalysts under ultrahigh vacuum (UHV) environment (pressures <10⁻⁷ Torr).⁹¹ With the implementation of ambient-pressure XPS at several synchrotron facilities it is now possible to study intermediates in common catalytic and electrocatalytic processes. The concept of differential pumping for moderate- or ambient-pressure XPS was first applied by Siegbahn and his colleagues in 1969 for investigation of gases at pressures of up to a few tenths of a Torr.⁹² In recent years the instrumental development of differentially pumped electron-energy analyzers equipped with fast multichannel detectors and access to the new generation of synchrotrons has opened new exciting possibilities,⁹³ such as studying chemical transformations on surfaces using photoemission under conditions that are much closer to realistic environments and therefore of direct relevance to catalysis.^{94–96} Figure 10 shows the setup for a moderate-pressure XPS instrument.⁹⁷ The key feature of a ambient-pressure XPS system is the differential pumping between the sample and the electron energy analyzer.^{95,97} The XPS signal level is strongly influenced by the flux of the X-ray source, the scattering of the photoelectrons by the gas phase, and the efficiency of the photoelectron collection by the

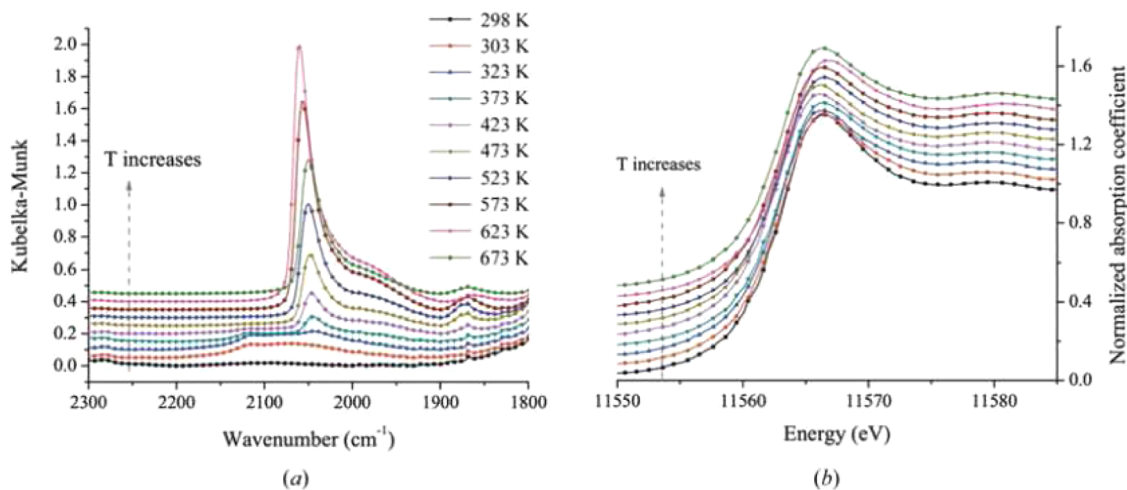


Figure 9. (a) DRIFTS and (b) Pt L₃ XANES spectra taken during the reduction of a 5 wt % Pt/Al₂O₃ catalyst in 5% H₂/He from room temperature to 400 °C. Reprinted with permission from ref 88. Copyright 2011 Wiley.

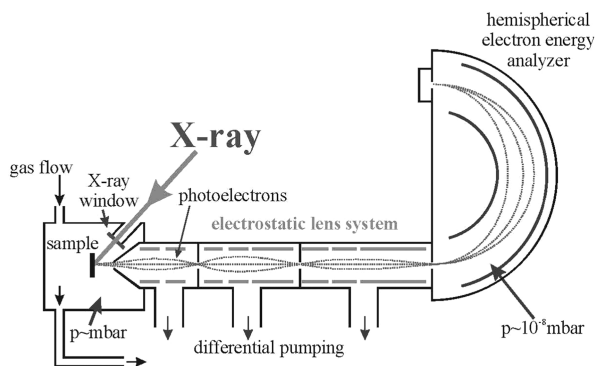


Figure 10. Ambient-pressure XPS setup (with permission of Ph.D. thesis author in ref 97).

spectrometer.^{95,97} For practical reasons, a highly intense synchrotron beam is necessary as the source of soft X-rays. The use of electrostatic lenses within the differential pumping stages substantially enhances the efficiency of the detection process.^{95,97} The main factor limiting the maximum working pressure in the sample cell is the scattering of low-energy photoelectrons by gas phase molecules. The operating pressure in modern analyzers can range up to 5–10 Torr,^{95,97} which is sufficient to study many chemical reactions that are associated with catalytic processes and will not occur under UHV environment.^{95,98}

At present ambient-pressure XPS has been used to follow the kinetics of surface reactions and to study reaction mechanisms.^{95,98} Figure 11 shows Ru 3d_{5/2} XPS spectra for the oxidation of Ru(001) collected at the ALS⁹⁹ with an electron-energy analyzer that has differential pumping stages similar to those shown in Figure 10.⁹⁷ The XPS spectra were recorded in a period of ~30 s and clearly show the growth of RuO_x. Several articles published by the Berkeley and Fritz-Haber laboratories nicely illustrate the uniqueness of moderate pressure high resolution XPS for in situ studies of Cu catalysts for methanol oxidation.⁹⁵ Ambient pressure XPS instruments with sub-

monolayer sensitivity are currently installed at several synchrotron facilities in Europe (BESSY, ELETTRA, MAX-LAB) and the U.S. (ALS, NSLS), and the technique starts to be widely applied in operando studies.^{95,98} The next major challenge is to shift the range of operating pressures up to 500 Torr or higher.^{95,98}

4. BRINGING CATALYSIS COMMUNITY TO SYNCHROTRONS

Despite their unique advantages for in situ catalytic studies, synchrotron techniques are often underutilized or unexplored by the catalysis community because of various perceived and real barriers. For example, the participation in synchrotron research would require access to beamtime facilities, fabrication of in situ reactors, and knowledge of beamline operations and data analysis, among other things. These requirements present significant barriers for research groups without previous synchrotron experience. Coordinated efforts are needed to assist new users, as well as to develop new capabilities for experienced users. One successful example is the Synchrotron Catalysis Consortium (SCC) consisting of catalysis researchers from academic, national, and industrial laboratories. Since its establishment in 2005, at the National Synchrotron Light Source at Brookhaven National Laboratory, the SCC team has coordinated significant efforts to promote the utilization of cutting-edge catalytic research through the following concerted efforts:

- Dedicated beamlines for XAS and XRD measurements.
- Dedicated in situ reactors for a variety of catalytic and electrocatalytic studies.
- Dedicated staff to assist experimental setup and data analysis.
- Training courses and help sessions provided by the SCC team members.
- Development of new techniques for catalytic and electrocatalytic research.

Using these concerted approaches the SCC team has built and/or tested several instruments for catalytic investigations:

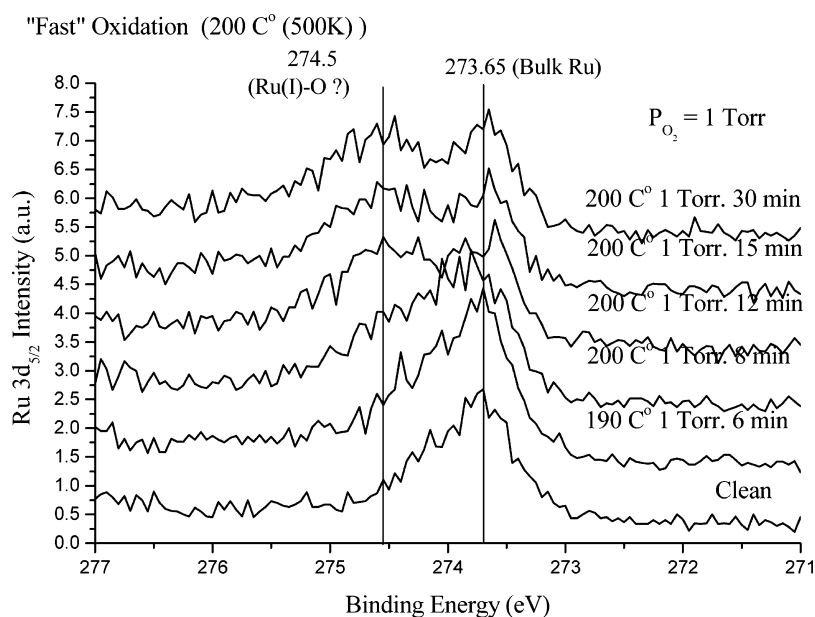


Figure 11. Ru 3d_{5/2} XPS spectra taken in situ during the oxidation of Ru(001) by 1 Torr of O₂ at 573K. (modified with permission from an unpublished figure from ref 99).

QEXAFS,¹⁰⁰ XAS-XRD,¹¹ XAS-DAFS,¹¹ XAS-DRIFTS,⁸⁸ and XAS-XRD-Raman.¹⁰¹ SCC members trained several hundreds new users and provided assistance to numerous catalysis research groups. The accomplishment of the SCC team demonstrates the critical importance of establishing national and international consortia to coordinate synchrotron research with the catalysis community.

Many synchrotron facilities have taken similar steps toward joining forces with regional catalysis user groups and developing new ways to organize catalysis community around synchrotron techniques. In the 1990s HASYLAB at DESY dedicated an EXAFS beamline for catalysis research. The beamline was equipped with an integrated laboratory and large space for building up in situ equipment, including gas lines and gas sensors. A similar trend can be found in at ESRF (e.g., dedicated facilities for in situ XAS at the Swiss-Norwegian beamline and DUBBLE where several techniques can be combined), SLS (SuperXAS beamline that allows users to monitor changes in catalysts in the subsecond scale with a QEXAFS monochromator), and the SAMBA beamline at SOLEIL.¹⁰² APS at Argonne National Laboratory has several beamlines with infrastructure for catalysis research and dedicated scientific staff to support catalysis users.

5. OUTLOOK AND OPPORTUNITIES

In the current Perspective we summarized several areas where we and others^{2,5,13,24} observe potentials for future progress in the field of combining synchrotron-based methods with complementary techniques for catalytic studies. Opportunities exist for new operando cell designs that enable more powerful applications of combined techniques to study homogeneous and heterogeneous catalysis in liquid phase, and liquid–solid interface, which are relatively less explored compared to the catalysis in solid phase or at the solid–gas interface.

More work is required to fully explore the potential of high energy resolution techniques: high energy resolution fluorescence detection (HERFD), X-ray emission spectroscopy (XES), and resonant inelastic X-ray scattering (RIXS), and their combination with the XAS method. These techniques, coupled with the high flux beamlines and fast time resolution data acquisition methods (Dispersive EXAFS and QEXAFS) are powerful tools for studying electronic structure of catalysts and probing their interactions with reactants and products.

Another capability that is currently in its infancy but is being rapidly developed at the synchrotron facilities over the world (Diamond, APS, NSLS-II) is the X-ray spectroscopy and imaging of individual nanoparticles under operando conditions. The motivation for this work is to be able to measure, quantitatively, the charge state, bonding distribution, strain within individual clusters, and correlate them with reactivity. Combining the analytical power of XAS methods to materials' charge state, bonding structure, and dynamics, this goal can be reached when the nanoprobe is available to study XAS in individual nanoparticles.

Despite the many advantages of combining complementary techniques in a single experiment, and many innovations that bring together techniques that were not possible to combine 5–10 years ago, the inherent limitation of such approach (not being able to combine all useful techniques in one experiment) will always remain. One such challenge is the need to overcome the nonlocal, ensemble-averaging nature of absorption and scattering methods.⁹⁴ Catalytic properties are strongly affected by size and shape of the nanoparticles, which exhibit a broad

range of sizes, shapes, and compositions in real processes. Therefore, there is a clear need to include electron microscopy and diffraction to the synchrotron-based set of tools for catalysis research. Within the currently used philosophy of combining instruments in a single experiment, this would require the installation of an electron microscope in the synchrotron end station, which represents a difficult but achievable goal. Another approach will require a paradigm shift from the “combination of techniques in a single experiment” to a “portable, versatile microreactor compatible with X-ray and electron probes”. As a first step toward that goal, de Groot et al. have recently carried out an in situ STXM study of a Fischer–Tropsch catalyst.³³ One particular aspect of this work that is appealing for the new approach is that the nanoreactor used by de Groot et al. was adapted from the cell originally used for high-resolution electron microscopy, and thus compatible for both.

Equally important to instrument development, well coordinated consortia with dedicated staff and in situ reaction cells are essential to make the synchrotron facilities available to the broader catalysis community. The close interactions between beamline scientists and catalysis researchers within the consortia will also promote instrument development tailored to enhance in situ catalytic studies.

AUTHOR INFORMATION

Corresponding Author

*E-mail: anatoly.frenkel@yu.edu (A.I.F.), rodriguez@bnl.gov (J.A.R.), jgchen@udel.edu (J.G.C.).

Funding

This work was supported by the U.S. Department of Energy Grant DE-FG02-05ER15688.

Notes

The authors declare no competing financial interest.

ACKNOWLEDGMENTS

The authors are grateful to the members and staff of the Synchrotron Catalysis Consortium (SCC), Drs. R. Adzic, S. Bare, E. Carino, J. Hanson, J. Hrbek, S. Hulbert, C.-C. Kao, N. Marinkovic, D. Mullins, S. Overbury, and Q. Wang for help in establishing and operating the SCC.

REFERENCES

- (1) Surnev, S.; Ramsey, M. G.; Netzer, F. P. *J. Phys.: Condens. Matter* **2001**, *13*, 11305.
- (2) Singh, J.; Lamberti, C.; van Bokhoven, J. A. *Chem. Soc. Rev.* **2010**, *39*, 4754–4766.
- (3) Herein, D. X-Ray Powder Diffraction. In *Handbook of Heterogeneous Catalysis*; Wiley-VCH: Weinheim, Germany, 2008.
- (4) Stavitski, E.; Beale, A. M.; Weckhuysen, B. M. *Catalyst Characterization-Heterogeneous*. In *Encyclopedia of Catalysis*; John Wiley & Sons, Inc.: Hoboken, NJ, 2002.
- (5) Beale, A. M.; Jacques, S. D. M.; Weckhuysen, B. M. *Chem. Soc. Rev.* **2010**, *39*, 4656–4672.
- (6) Stavitski, E.; Weckhuysen, B. M. *Chem. Soc. Rev.* **2010**, *39*, 4615–4625.
- (7) Clausen, B. S.; Gråbæk, L.; Steffensen, G.; Hansen, P. L.; Topsøe, H. *Catal. Lett.* **1993**, *20*, 23–36.
- (8) Clausen, B. S. *Catal. Today*. **1998**, *39*, 293–300.
- (9) Grunwaldt, J.-D.; Clausen, B. S. *Top. Catal.* **2002**, *18*, 37–43.
- (10) Shannon, I. J.; Maschmeyer, T.; Sankar, G.; Thomas, J. M.; Oldroyd, R. D.; Sheehy, M.; Madill, D.; Waller, A. M.; Townsend, R. P. *Catal. Lett.* **1997**, *44*, 23–27.

- (11) Frenkel, A. I.; Wang, Q.; Marinkovic, N.; Chen, J. G.; Barrio, L.; Si, R.; Cámara, A. L. p.; Estrella, A. M.; Rodriguez, J. A.; Hanson, J. C. *J. Phys. Chem. C* **2011**, *115*, 17884–17890.
- (12) Weckhuysen, B. M. *Phys. Chem. Chem. Phys.* **2003**, *5*, 4351–4360.
- (13) Tinnemans, S. J.; Mesu, J. G.; Kervinen, K.; Visser, T.; Nijhuis, T. A.; Beale, A. M.; Keller, D. E.; van der Eerden, A. M. J.; Weckhuysen, B. M. *Catal. Today* **2006**, *113*, 3–15.
- (14) Beale, A. M.; van der Eerden, A. M. J.; Jacques, S. D. M.; Leynaud, O.; O'Brien, M. G.; Meneau, F.; Nikitenko, S.; Bras, W.; Weckhuysen, B. M. *J. Am. Chem. Soc.* **2006**, *128*, 12386–12387.
- (15) Mesu, J. G.; van der Eerden, A. M. J.; de Groot, F. M. F.; Weckhuysen, B. M. *J. Phys. Chem. B* **2005**, *109*, 4042–4047.
- (16) Tromp, M.; Sietsma, J. R. A.; van Bokhoven, J. A.; van Strijdonck, G. P. F.; van Haaren, R. J.; van der Eerden, A. M. J.; van Leeuwen, P. W. N. M.; Koningsberger, D. C. *Chem. Commun.* **2003**, 128–129.
- (17) Nikitenko, S.; Beale, A. M.; van der Eerden, A. M. J.; Jacques, S. D. M.; Leynaud, O.; O'Brien, M. G.; Detollenaere, D.; Kaptein, R.; Weckhuysen, B. M.; Bras, W. *J. Synchrotron Radiat.* **2008**, *15*, 632–640.
- (18) Newton, M. A.; Belver-Coldeira, C.; Martínez-Arias, A.; Fernández-García, M. *Nat. Mater.* **2007**, *6*, 528–532.
- (19) Newton, M. A.; Dent, A. J.; Fiddy, S. G.; Jyoti, B.; Evans, J. *Catal. Today* **2007**, *126*, 64–72.
- (20) Newton, M. *Topics in Catalysis* **2009**, *52*, 1410–1424.
- (21) Newton, M. A.; Michiel, M. D.; Kubacka, A.; Fernández-García, M. *J. Am. Chem. Soc.* **2010**, *132*, 4540–4541.
- (22) Newton, M. A.; Chapman, K. W.; Thompson, D.; Chupas, P. J. *J. Am. Chem. Soc.* **2012**, *134*, 5036–5039.
- (23) Chupas, P. J.; Chapman, K. W.; Jennings, G.; Lee, P. L.; Grey, C. P. *J. Am. Chem. Soc.* **2007**, *129*, 13822–13824.
- (24) Bentrup, U. *Chem. Soc. Rev.* **2010**, *39*, 4718–4730.
- (25) Bare, S. R.; Mickelson, G. E.; Modica, F. S.; Ringwelski, A. Z.; Yang, N. *Rev. Sci. Instrum.* **2006**, *77*, 023105.
- (26) Grunwaldt, J. D.; Caravati, M.; Hannemann, S.; Baiker, A. *Phys. Chem. Chem. Phys.* **2004**, *6*, 3037–3047.
- (27) Moggridge, G. D.; Schroeder, S. L. M.; Lambert, R. M.; Rayment, T. *Nucl. Instrum. Methods Phys. Res., Sect. B* **1995**, *97*, 28–32.
- (28) Newton, M. A.; Jyoti, B.; Dent, A. J.; Fiddy, S. G.; Evans, J. *Chem. Commun.* **2004**, 2382–2383.
- (29) Beale, A. M.; van der Eerden, A. M. J.; Kervinen, K.; Newton, M. A.; Weckhuysen, B. M. *Chem. Commun.* **2005**, 3015–3017.
- (30) Ginder-Vogel, M.; Landrot, G.; Fischel, J. S.; Sparks, D. L. *Proc. Natl. Acad. Sci. U.S.A.* **2009**, *106*, 16124–16128.
- (31) Golovchak, R.; Kovalskiy, A.; Shpotyuk, O.; Jain, H. *Appl. Phys. Lett.* **2011**, *98*, 171905.
- (32) Chan, E. M.; Marcus, M. A.; Fakra, S.; ElNaggar, M.; Mathies, R. A.; Alivisatos, A. P. *J. Phys. Chem. A* **2007**, *111*, 12210–12215.
- (33) de Smit, E.; Swart, I.; Creemer, J. F.; Hoveling, G. H.; Gilles, M. K.; Tyliszczak, T.; Kooyman, P. J.; Zandbergen, H. W.; Morin, C.; Weckhuysen, B. M.; de Groot, F. M. F. *Nature* **2008**, *456*, 222–225.
- (34) Ferrer, S.; Petroff, Y. *Surf. Sci.* **2002**, *500*, 605–627.
- (35) Madey, T. E.; Pelhos, K.; Wu, Q.; Barnes, R.; Ermanoski, I.; Chen, W.; Kolodziej, J. J.; Rowe, J. E. *Proc. Natl. Acad. Sci. U.S.A.* **2002**, *99*, 6503–6508.
- (36) Zubavichus, V.; L. Slovokhotov, Y. *Russ. Chem. Rev.* **2001**, *70*, 373–403.
- (37) Burch, R. *Phys. Chem. Chem. Phys.* **2006**, *8*, 5483–5500.
- (38) Wang, X.; Rodriguez, J. A.; Hanson, J. C.; Gamarra, D.; Martínez-Arias, A.; Fernández-García, M. *J. Phys. Chem. B* **2005**, *110*, 428–434.
- (39) Wang, X.; Rodriguez, J. A.; Hanson, J. C.; Perez, M.; Evans, J. J. *Chem. Phys.* **2005**, *123*, 221101.
- (40) Rodriguez, J. A.; Hanson, J. C.; Wen, W.; Wang, X.; Brito, J. L.; Martínez-Arias, A.; Fernández-García, M. *Catal. Today* **2009**, *145*, 188–194.
- (41) Wang, Q.; Hanson, J. C.; Frenkel, A. I. *J. Chem. Phys.* **2008**, *129*, 42
- (42) Barrio, L.; Estrella, M.; Zhou, G.; Wen, W.; Hanson, J. C.; Hungria, A. B.; Hornés, A.; Fernández-García, M.; Martínez-Arias, A.; Rodriguez, J. A. *J. Phys. Chem. C* **2010**, *114*, 3580–3587.
- (43) Rodriguez, J. A. *Catal. Today* **2011**, *160*, 3–10.
- (44) Fu, Q.; Saltsburg, H.; Flytzani-Stephanopoulos, M. *Science* **2003**, *301*, 935–938.
- (45) Schwartz, V.; Mullins, D. R.; Yan, W.; Chen, B.; Dai, S.; Overbury, S. H. *J. Phys. Chem. B* **2004**, *108*, 15782–15790.
- (46) Wang, X.; Rodriguez, J.; Hanson, J.; Gamarra, D.; Martínez-Arias, A.; Fernández-García, M. *Top. Catal.* **2008**, *49*, 81–88.
- (47) Sasaki, K.; Wang, J. X.; Balasubramanian, M.; McBreen, J.; Uribe, F.; Adzic, R. R. *Electrochim. Acta* **2004**, *49*, 3873–3877.
- (48) Sasaki, K.; Adzic, R. R. *Synchrotron Radiat. News* **2009**, *22*, 17–21.
- (49) Erickson, E. M.; Thorum, M. S.; Vasić, R.; Marinković, N. S.; Frenkel, A. I.; Gewirth, A. A.; Nuzzo, R. G. *J. Am. Chem. Soc.* **2011**, *134*, 197–200.
- (50) Weir, M. G.; Myers, V. S.; Frenkel, A. I.; Crooks, R. M. *ChemPhysChem* **2010**, *11*, 2942–2950.
- (51) Kowal, A.; Li, M.; Shao, M.; Sasaki, K.; Vukmirovic, M. B.; Zhang, J.; Marinkovic, N. S.; Liu, P.; Frenkel, A. I.; Adzic, R. R. *Nat. Mater.* **2009**, *8*, 325–330.
- (52) Stephens, I. E. L.; Bondarenko, A. S.; Gronbjerg, U.; Rossmeisl, J.; Chorkendorff, I. *Energy Environ. Sci.* **2012**, *5*, 6744–6762.
- (53) Rettew, R. E.; Allam, N. K.; Alamgir, F. M. *ACS Appl. Mater. Interfaces* **2011**, *3*, 147–151.
- (54) Cheng, S.; Rettew, R. E.; Sauerbrey, M.; Alamgir, F. M. *ACS Appl. Mater. Interfaces* **2011**, *3*, 3948–3956.
- (55) Esposito, D. V.; Hunt, S. T.; Stottlemeyer, A. L.; Dobson, K. D.; McCandless, B. E.; Birkmire, R. W.; Chen, J. G. *Angew. Chem., Int. Ed.* **2010**, *49*, 9859–9862.
- (56) Esposito, D. V.; Forest, R. V.; Chang, Y.; Hou, S.; McCandless, B. E.; Gaillard, N.; Lee, K. H.; Birkmire, R. W.; Chen, J. G. *Energy Environ. Sci.* **2012**, *5* (10), 9091–9099.
- (57) Heinemann, H., *Development of Industrial Catalysis*; Wiley-VCH: Weinheim, Germany, 1997.
- (58) Bartholomew, C. H.; Farrauto, R. J. *Fundamentals of Industrial Catalytic Processes*, 2nd ed.; Wiley-Aiche: New York, 2005.
- (59) Hagen, J. *Industrial Catalysis: A Practical Approach*; Wiley-VCH: Weinheim, Germany, 2006.
- (60) Bergeret, G. *Structure and Morphology. X-ray Powder Diffraction*; Wiley-VCH: Weinheim, Germany, 1997.
- (61) Chorkendorff, I.; Niemantsverdriet, J. W. *Concepts of Modern Catalysis and Kinetics*, 2nd ed.; Wiley-VCH: Weinheim, Germany, 2007.
- (62) Norby, P.; Hanson, J. C. *Catal. Today* **1998**, *39*, 301–309.
- (63) Sankar, G.; Thomas, J. M. *Top. Catal.* **1999**, *8*, 1–21.
- (64) Stragier, H.; Cross, J. O.; Rehr, J. J.; Sorensen, L. B.; Bouldin, C. E.; Woicik, J. C. *Phys. Rev. Lett.* **1992**, *69*, 3064–3067.
- (65) Frenkel, A. I.; Kolobov, A. V.; Robinson, I. K.; Cross, J. O.; Maeda, Y.; Bouldin, C. E. *Phys. Rev. Lett.* **2002**, *89*, 285503.
- (66) Grunwaldt, J.-D.; Kimmerle, B.; Baiker, A.; Boye, P.; Schroer, C. G.; Glatzel, P.; Borca, C. N.; Beckmann, F. *Catal. Today* **2009**, *145*, 267–278.
- (67) Grunwaldt, J.-D.; Schroer, C. G. *Chem. Soc. Rev.* **2010**, *39*, 4741–4753.
- (68) Schroer, C. G.; Kuhlmann, M.; Gunzler, T. F.; Lengeler, B.; Richwin, M.; Griesebock, B.; Lutzenkirchen-Hecht, D.; Frahm, R.; Ziegler, E.; Mashayekhi, A.; Haefner, D. R.; Grunwaldt, J.-D.; Baiker, A. *Appl. Phys. Lett.* **2003**, *82*, 3360–3362.
- (69) Jones, K. W.; Feng, H.; Lanzirrotti, A.; Mahajan, D. *Top. Catal.* **2005**, *32*, 263–272.
- (70) Grunwaldt, J.-D.; Hannemann, S.; Schroer, C. G.; Baiker, A. *J. Phys. Chem. B* **2006**, *110*, 8674–8680.
- (71) Kimmerle, B.; Grunwaldt, J.-D.; Baiker, A.; Glatzel, P.; Boye, P.; Stephan, S.; Schroer, C. G. *J. Phys. Chem. C* **2009**, *113*, 3037–3040.
- (72) Frenkel, A. I.; Kleefeld, O.; Wasserman, S. R.; Sagi, I. *J. Chem. Phys.* **2002**, *116*, 9449–9456.

- (73) Wang, X. Q.; Hanson, J. C.; Frenkel, A. I.; Kim, J. Y.; Rodriguez, J. A. *J. Phys. Chem. B* **2004**, *108*, 13667–13673.
- (74) Kim, J. Y.; Rodriguez, J. A.; Hanson, J. C.; Frenkel, A. I.; Lee, P. L. *J. Am. Chem. Soc.* **2003**, *125*, 10684–10692.
- (75) Rodriguez, J. A.; Hanson, J. C.; Frenkel, A. I.; Kim, J. Y.; Perez, M. *J. Am. Chem. Soc.* **2002**, *124*, 346–354.
- (76) Boudart, M. *Principles of Heterogeneous Catalysis*; Wiley-VCH: Weinheim, Germany, 1997.
- (77) Campbell, C. T. *Top. Catal.* **1994**, *1*, 353–366.
- (78) Ryczkowski, J. *Catal. Today*. **2001**, *68*, 263–381.
- (79) Chuang, S.; Guzman, F. *Top. Catal.* **2009**, *52*, 1448–1458.
- (80) Xu, W.; Si, R.; Senanayake, S. D.; Llorca, J.; Idriss, H.; Stacchiola, D.; Hanson, J. C.; Rodriguez, J. A. *J. Catal.* **2012**, *291*, 117–126.
- (81) Burch, R.; Goguet, A.; Meunier, F. C. *Appl. Catal., A* **2011**, *409–410*, 3–12.
- (82) Rodriguez, J. A.; Truong, C. M.; Goodman, D. W. *J. Chem. Phys.* **1992**, *96*, 7814–7825.
- (83) Xu, M.; Gao, Y.; Wang, Y.; Woll, C. *Phys. Chem. Chem. Phys.* **2010**, *12*, 3649–3652.
- (84) Baron, M.; Abbott, H.; Bondarchuk, O.; Stacchiola, D.; Uhl, A.; Shaikhtudinov, S.; Freund, H.-J.; Popa, C.; Ganduglia-Pirovano, M. V.; Sauer, J. *Angew. Chem., Int. Ed.* **2009**, *48*, 8006–8009.
- (85) Bañares, M. A.; Mestl, G. Structural Characterization of Operating Catalysts by Raman Spectroscopy. In *Advances in Catalysis*; Bruce, C. G., Helmut, K., Eds.; Academic Press: New York, 2009; Vol. 52, pp 43–128.
- (86) Drago, R. S. *Physical Methods for Chemists*, 2nd ed.; Saunders: New York, 1992.
- (87) Newton, M. A.; van Beek, W. *Chem. Soc. Rev.* **2010**, *39*, 4845–4863.
- (88) Marinkovic, N. S.; Wang, Q.; Frenkel, A. I. *J. Synchrotron. Radiat.* **2011**, *18*, 447–455.
- (89) Briois, V.; Lützenkirchen-Hecht, D.; Villain, F.; Fonda, E.; Belin, S.; Griesebock, B.; Frahm, R. *J. Phys. Chem. A* **2004**, *109*, 320–329.
- (90) Wragg, D. S.; Johnsen, R. E.; Balasundaram, M.; Norby, P.; Fjellvåg, H.; Grønvold, A.; Fuglerud, T.; Hafizovic, J.; Vistad, Ø. B.; Akporiaye, D. *J. Catal.* **2009**, *268*, 290–296.
- (91) White, M. G. *Heterogeneous Catalysis*; Prentice Hall: Englewood Cliffs, NJ, 1990.
- (92) Siegbahn, K. e. a., *ESCA Applied to Free Molecules*; North-Holland: Amsterdam, The Netherlands, 1969.
- (93) Frank Ogletree, D.; Bluhm, H.; Hebenstreit, E. D.; Salmeron, M. *Nucl. Instrum. Methods Phys. Res., Sect. A* **2009**, *601*, 151–160.
- (94) Tao, F.; Salmeron, M. *Science* **2011**, *331*, 171–174.
- (95) Salmeron, M.; Schlögl, R. *Surf. Sci. Rep.* **2008**, *63*, 169–199.
- (96) Bluhm, H.; Ogletree, D. F.; Fadley, C. S.; Hussain, Z.; Salmeron, M. *J. Phys.: Condens. Matter* **2002**, *14*, L227.
- (97) Kleimenov, E. Ph.D. Dissertation, Technischen Universität Berlin, Berlin, Germany, 2005.
- (98) Starr, D. E.; Bluhm, H.; Liu, Z.; Knop-Gericke, A.; Havecker, M. *Application of Ambient Pressure X-Ray Photoelectron Spectroscopy for the In-Situ Investigation of Heterogeneous Catalytic Reactions*. Wiley: New York, 2012.
- (99) Nambu, A.; Rodriguez, J. A.; Hrbek, J., in preparation.
- (100) Khalid, S.; Caliebe, W.; Siddons, P.; So, I.; Clay, B.; Lenhard, T.; Hanson, J.; Wang, Q.; Frenkel, A. I.; Marinkovic, N.; Hould, N.; Ginder-Vogel, M.; Landrot, G. L.; Sparks, D. L.; Ganjoo, A. *Rev. Sci. Instrum.* **2010**, *81*, 015105–015112.
- (101) Patlolla, A.; Carino, E. V.; Ehrlich, S. N.; Stavitski, E.; Frenkel, A. I. *ACS Catal.* **2012**, *2*, 2216–2223.
- (102) Grunwaldt, J.-D.; Frenkel, A. I. *Synchrotron Radiat. News* **2009**, *22*, 2–4.